Energy-Efficiency of Cooperative MIMO Wireless Systems

By

Daniel Muchiri

Submitted to the graduate degree program in Electrical Engineering and Computer Science and the
Graduate Faculty of the University of Kansas
in partial fulfillment of the requirements for the degree of
Master of Science

Dr. Lingjia Liu, Chairperson

Committee members

Dr. Erik Perrins

Dr. Sarah Seguin

Dr. Christopher Allen

Date defended: December 16, 2014

The Masters thesis Committee for Daniel Muchiri certifies
that this is the approved version of the following masters thesis :

Energy-Efficiency of Cooperative MIMO Wireless Systems

Committee members

Dr. Lingjia Liu, Chairperson

Dr. Erik Perrins

Dr. Sarah Seguin

Dr. Christopher Allen

Date approved: December 16, 2014

Abstract

Increasing focus on global warming has challenged the scientific community to develop ways to mitigate its adverse effects. This is more so important as different technologies become an integral part of daily human life. Mobile wireless networks and mobile devices form a significant part of these technologies. It is estimated that there are over four billion mobile phone subscribers worldwide and this number is still growing as more people get connected in developing countries [1]. In addition to the growing number of subscribers, there is an explosive growth in high data applications among mobile terminal users. This has put increased demand on the mobile network in terms of energy needed to support both the growth in subscribers and higher data rates. The mobile wireless industry therefore has a significant part to play in the mitigation of global warming effects. To achieve this goal, there is a need to develop and design energy efficient communication schemes for deployment in future networks and upgrades to existing networks. This is not only done in the wireless communication infrastructure but also in mobile terminals. In this thesis a practical power consumption model which includes circuit power consumption from the different components in a transceiver chain is analyzed. This is of great significance to practical system design when doing energy consumption and energy efficiency analysis. The proposed power consumption model is then used to evaluate the energy efficiency in the context of cooperative Multiple Input Multiple Output (MIMO) systems.

Acknowledgements

I would like to thank my committee members especially Dr. Lingjia Liu who has been my advisor during my time at the University of Kansas for his professional guidance, support and patients during the writing of this thesis. I would also like to thank Dr. Sarah Seguin, Dr. Erik Perrins and Dr. Christopher Allen for their time and kindness to serve on my thesis committee, and helpful advice towards the fulfillment of my thesis. I also want to thank Dr. Liu's research group members for their advice and feedback at different levels of my research especially Rachad Atat, Yan Li, Farhad Mahmood and Hao Chen for there enormous help during the writing of my thesis. Lastly I would like to thank my parents, siblings and all my friends for their continued encouragement and support during the course of my studies at the University of Kansas.

Contents

List of Figures

List of Tables

Chapter 1

Introduction

1.1 Motivation

In the current decade, mobile-cellular penetration has reached a peak never before seen. Although the penetration rate is flattening, reaching a peak of 96 percent by the end of 2013, the growth of mobile-broadband can still be thought of as being in its infancy with growth rates of around 40 percent annually between 2010 and 2013. According to ITU estimates, there will be 6.8 billion mobile-cellular subscriptions by the end of 2013 almost as many as there are people on the planet [2]. Of this about 2.7 billion people are using Internet worldwide therefore there still exist a gap between those with mobile-cellular subscriptions and those who have access to mobile broadband. As a result, Ericsson forecast that by 2018 there will be as many as 6.5 billion mobile-broadband subscriptions, almost as many as there were mobile-cellular subscriptions in 2013 [2]. With this many mobile subscriptions and almost all people on earth leaving somewhere within reach of a mobile-cellular signal, the mobile network infrastructure needed to accomplish this is staggering. In 2007 there were about 3.3 million radio base stations (RBS) sites in operation. In 2009 the number was up to 4.6 million sites, counting all standards [3]. With the continued growth of mobile-broadband services, this number is bound to increase as more and more radio base stations go on air and with it the overall energy consumption of the mobile network industry will increase.

The rapid evolution of information and communication technology (ICT) and projected growth in mobile data services has consequently led to the increase in energy consumption of ICT systems used. This increase in energy consumption has resulted in making mobile operators one of the top energy consumers in the world. Global consultants Gartner estimate that ICTs accounts for approximately 0.86 metric gigatonnes of carbon emissions annually, or just about 2 percent of global carbon emissions [4]. The International Telecommunication Union (ITU) has estimated the contribution of ICTs (excluding the broadcasting sector) to climate change at between 2 percent and 2.5 percent of total global carbon emissions. The main contributing sectors within the ICT industry include the energy requirements of PCs and monitors 40%, data centers, which contribute a further 23%, and fixed and mobile telecommunications that contribute 24% of the total emissions [4].

Due to the continued deployment of 3G technologies in developing countries and 4G systems in the western world, the growth in energy consumption is bound to keep increasing [5]. This increased energy consumption is reflected in high electric bills for mobile phone operators with the largest contribution coming from the mobile base stations (BS). At the BS more than 50% of the total energy is consumed by the radio access portion with the power amplifier (PA) using over 50% of this energy [5]. Also in the mature European markets, approximately 18% of the operation expenditure is due to the energy bill therefore, for mobile operators energy efficiency (EE) will not only play a great part in reducing their carbon foot print but also has significant economic benefits for them.

Mobile terminals (MT) such as mobile phones, have become an integral part of our lives in the resent past, transforming our lives and giving us the freedom to talk, work, watch and listen on the move. However this freedom is limited on the battery life, unplug from the mains and the freedom only last as long as the energy held within the device's battery lasts. Battery life compounded with the increasing use of energy hungry mobile-broadband applications on our MTs has focused attention on how to more efficiently use energy on the MT [6]. This is more so important since the development of the battery has not kept up with the growing demands in all major industries

not only the ICT industry. For example the lead-acid car batteries have been around for approximately 150 years and the lithium-ion battery, which powers most modern gadgets, was invented in the 1970s. It is no surprise then that the increased use by mobile phone users of energy hungry applications such as video streaming, video sharing, mobile TV, 3D services, interactive video and many more, has led to increased focus and research on how the radio access network on the mobile terminal is designed so as to reduce the overall energy drain on the battery and thus extend battery life.

Also with the increased growth of high-data-rate applications such as those mentioned above, EE in wireless networks has drawn increasing interest from the research community internationally. The research is focused in areas such as low power circuit design, high-efficiency PA and digital signal processing (DSP) technologies, advanced cooling systems, adequate EE metric and energy consumption models, cell-size deployment, various relay and cooperative communications techniques, adaptive traffic pattern and load variation algorithms, energy efficient network resource management, as well as MIMO and OFDM techniques [5], [7].

1.2   Background and Related Work

As observed in [2], [4] and [5], with the increased deployment of mobile networks to cover more and more of the worlds population and the explosive growth of high data rate applications, EE in wireless communication has drawn increasing attention from the research community world wide and rightly so. As a result, there are a number of international research efforts focused on energy efficient wireless communications such as: Green radio project, EARTH project, OPERA-Net project and eWin project [5].

A novel EE metric is of great importance when it comes to the overall design of an energy-efficient network as it relates directly to the optimization decision across all protocol layers [5]. In current literature, several different EE metrics have been used with the most popular being bits-per-joule which is defined as the system throughput for unit-energy consumption. In some of

the literature considered in [5], the energy consumption models only consider the transmit power associated with the data transmission rate; however, transmit power is only a part of the overall energy budget and the same paper concludes that when the energy consumption of other parts such as the transceiver circuit power consumption is taken into account such naïve energy-efficiency schemes might not be appropriate.

The increasing need for higher data rates in wireless communication systems needed to support the ever increasing number of data hungry applications, has brought about an increased interest in Multiple Input Multiple Output (MIMO) system. This is because MIMO systems have been shown to support higher data rates under the same transmit power budget and bit error rate performance requirements as a Single Input Single Output (SISO) system [8]. The use of multiple number of antennas is employed for the purpose of obtaining multiple signal paths which are exploited to combat fading by spatial multiplexing techniques or used to increase link capacity by allowing transmission of different data streams from different antennas. That is to say higher data through-put and more reliable communication can be ensured. The transmit power consumption for each antenna is also extremely low in massive MIMO systems according to [8]. Common models used in related work on spectral and energy efficiency that consider transmit power only indicate that the increment of the number of transmit antennas induces bigger data rate and energy efficiency performance. However as the number of antennas increase in MIMO systems, so does the number of circuit hardware, hence the circuit power consumption would be increased by a factor of the number of antennas [8]. This need for higher data rates together with the increased awareness on global warming has raised the question of whether MIMO systems are more energy efficient than SISO systems when the extra circuitry due to the increased number of antennas is considered in the overall energy consumption of the system. It is shown in [9] that when circuit power is taken into account there exist a crossover in the transmission rate with respect to EE between MIMO and Single Input Multiple Output (SIMO) below which SIMO is more energy efficient and above it MIMO is more energy efficient. In [8] MIMO energy efficiency as compared to SISO is evaluated with the aim of analyzing what effect the distance of propagation has on the overall efficiency. It

4

concludes that MIMO systems are not always more energy efficient than SISO systems at short distances and lays out different conditions when there is a threshold distance below which the SISO system outperforms the MIMO system in terms of energy efficiency. It is also shown that even when the energy consumption of the local information exchange for cooperation is considered, MIMO still outperforms direct transmission as long as the transmission distances are larger than a given threshold.

Multiple antennas at the transmitter and receiver are used to achieve both transmit and receive diversity by providing multiple signal paths. It is assumed that for the case of transmit diversity the transmitter knows the channel. For practical implementations of Long Term Evolution (LTE)-Advance systems, the feedback framework used since the early 3GPP releases entails the receiver measuring the down link (DL) channel through measurement reference signals and feeding back the Channel State Information (CSI) in the form of recommended transmission formats which include: Rank indicator (RI), Precoding Matrix Indicator (PMI) and Channel quality indicator (CQI) [10], [11]. These enable the transmitter to know the channel state information during data transfer. From this, it is clear that the definition of "throughput" affects the accuracy of the EE metric. Since not all transmitted data is information bits, not all transmitted data should be considered into the overall system throughput [5]. That is to say there is some overhead associated with data transmission over a wireless channel. Such overhead bits may include: header required in different protocols, signaling information, destroyed packets and duplicate packets. In [12], the energy consumption of training sequences for channel estimation is considered. It is shown that the optimal power allocation for pilot and data symbol in terms of EE can reduce transmit power consumption by 84.5% compared with optimal power allocation scheme for maximizing the capacity. A trade-off among transmission energy, circuit energy, and transmission time is investigated for different modulation schemes in [13]. Here it is shown that for uncoded systems, by optimizing the transmission time and the modulation parameters, up to 80% energy savings is achievable over non-optimized systems. For coded systems, it is shown that the benefit of coding varies with the transmission distance and the underlying modulation schemes. Energy-efficient

5

power adaptation in frequency-selective channels is addressed in [14]. Here results show that OFDM systems demonstrate improved energy savings with energy optimal link adaptation and a fundamental trade-off between energy-efficient and spectrum-efficient transmission is illustrated. Adaptive switching between MIMO and SIMO is studied in [9]. In this it is shown that there exists a crossover point on the transmission rate below which SIMO consumes less power than MIMO when circuit power is included. This crossover point is found to be an increasing function of the circuit power, the number of receive antennas and channel correlation. All of which increase the potential energy savings resulting from mode switching. [9] further proposes an adaptive mode switching algorithm combined with rate selection to maintain a user's target throughput while achieving energy efficiency.

This shows that the different methods of modeling the energy consumption of a wireless communication system have significant impact on the bits-per-Joule metric. This forms a basis for the importance of setting up a less simplistic energy consumption model which is done in this paper.

Relay and cooperative networks are also a strong area of focus when it comes to improving EE for mobile wireless networks. One of the ways that relay networks save energy is by reducing path loss due to shorter transmission distance and the potential to generate less interference due to low transmission power [5]. In [9], the advantages of relay transmission are examined with transmission delay and energy consumption of relay nodes both being considered. unlike in pure relay systems, energy savings for cooperative networks comes from the diversity that results from cooperation since each cooperative node can act as both an information source and a relay. In [8] it is shown that although cooperative diversity does offer energy savings, this savings are countered at short distances where direct communication is preferred over distributed space-time coding since using relays adds more energy consumption countering the transmission energy savings gained.

In [15] it is shown that there is a significant energy saving when cooperative ad hoc networks are used. This cooperative ad hoc network setup also leads to improved data rates for the distribution of common content to multiple receiving devices (MTs). Models used in [15] have single antenna scenarios and power consumption is not broken down to the various components found within the

6

transceiver, and as previously mentioned different methods of modeling the energy consumption have significant impact on the overall EE metric.

Therefore in this paper I will break down the circuit power to the various components in the RF chain and extend the work to cooperative MIMO systems with an initial setup such that the transmitter will have four antennas and the receiver will have two antennas. Also, a look at the gain in energy efficiency as the number of antennas is increased is also evaluated. In addition, the EE metric used will be the inverse of the commonly used bits-per-Joule metric, that is joules-per-bit, showing how much energy is spent in the transmission of one informational bit.

Chapter 2

System Model

2.1 General System Model

The cooperative system model is shown in figure 2.1. The model consists of K cooperating MTs in the range of a BS. The BS is connected via wired mobile core network to the server that holds the common content to be distributed. The BS sends the content to the MTs either via unicasting or multicasting on the long range (LR) links. MTs can communicate with each other via unicasting or multicasting over the short range (SR) links [15].

The transmit and receive antenna model is depicted in 2.2. In this we have the BS with $N_t \geq 1$ transmit (Tx) antennas and the MT with $N_r \geq 1$ receive (Rx) antennas. The power is assumed to be evenly distributed on the transmitting antennas on the BS and when a MT is retransmitting to other MTs in its neighborhood.

2.2 Parameters and Variables

The parameters affecting the energy consumption in the scenarios studied in this paper are defined as: $P_{out:BS}$ is the transmit power at the BS, $P_{PA:BS}$ the power amplifier power consumption at the BS, $P_{dac:BS}$ the power consumption from a Digital to Analog Converter (DAC) at the BS, $P_{filt:BS}$ the power consumption by the filter at the BS, $P_{syn:BS}$ the power consumption by the frequency
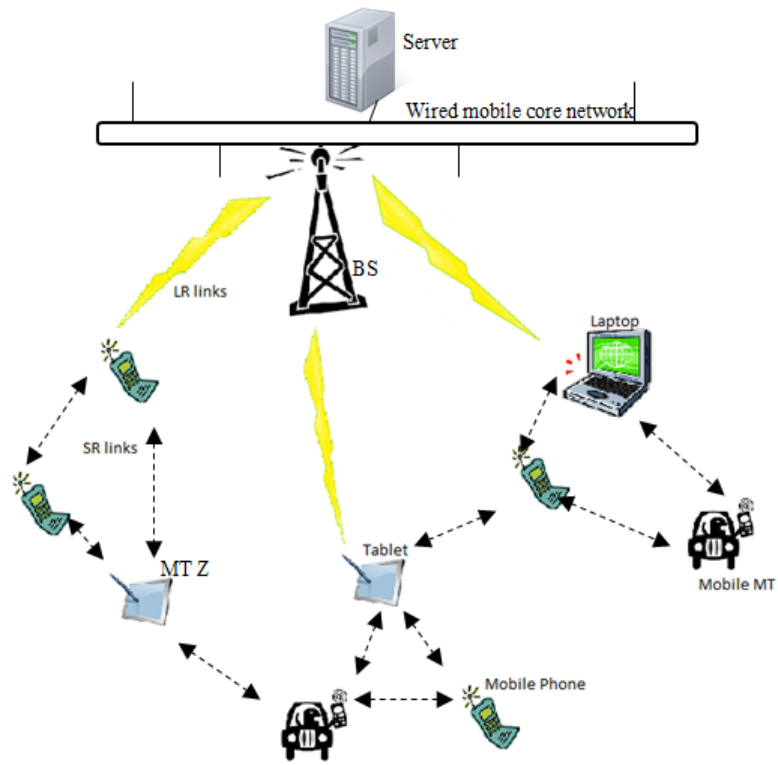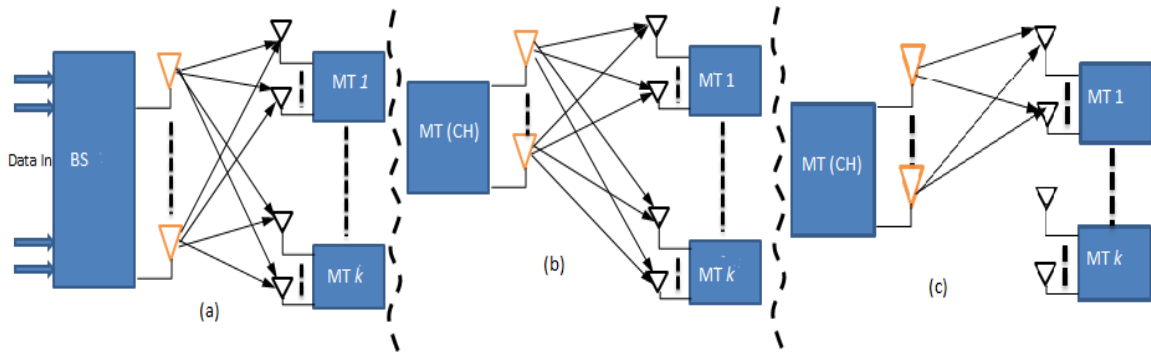
Figure 2.1: General system model

Figure 2.2: MIMO system model (a) BS multicasting scenario (b) MT multicasting scenario (c) MT unicasting scenario

synthesizer at the BS, $P_{sta:BS}$ the idle/static power consumption (Baseband interface) at the BS, $\sigma_{feed:BS}$ lossy factors of antenna feeder at BS, $\sigma_{DC:BS}$ lossy factors of DC-DC power supply at the BS, $\sigma_{MS:BS}$ lossy factors of main power supply at the BS, $\sigma_{cool:BS}$ lossy factors of the active cooling system at the BS, $P_{out:MT,Tx}$ is the transmit power at the MT during transmission, $P_{PA:MT,Tx}$ the power amplifier power consumption at the MT during transmission, $P_{dac:MT,Tx}$ the power consumption from a DAC at the MT during transmission, $P_{filt:MT,Tx}$ the power consumption by the filter at the MT during transmission, $P_{syn:MT,Tx}$ the power consumption by the frequency synthesizer at the MT during transmission, $P_{sta:MT,Tx}$ the idle/static power consumption (Baseband interface) at the MT during transmission, $P_{mix:MT,Tx}$ the power consumption by the mixer at the MT during transmission, $P_{adc:MT,Rx}$ the power consumption for an Analog to Digital Converter (ADC) at the MT during reception, $P_{filt:MT,Rx}$ the power consumption by the filter at the MT during reception, $P_{IFA:MT,Rx}$ the power consumption of the Intermediate Frequency Amplifier (IFA) at the MT during reception, $P_{mix:MT,Rx}$ the power consumption by the mixer at the MT during reception, $P_{LNA:MT,Rx}$ the power consumption by the Low Noise Amplifier (LNA) at the MT during reception, $P_{syn:MT,Rx}$ the power consumption by the frequency synthesizer at the MT during reception and K is the number of requesting MTs interested in the same content. Additional parameters and variables as relates to the data rates are : S_T the size in bits of the content of common interest to be distributed to all MTs. $R_{L,k}$ is the transmission rate on the Long Range (LR) link when unicasting from the BS to MTk, $R_{S,kj}$ the transmission rate on the Sort Range (SR) link from MTk to MTj, $S_R(m)$ remaining data, in bits, at the mth channel realization and m_T is the number of channel variations until the whole content of size S_T is distributed.

The P_t and P_r total transmit and receive power respectively over the air measured at the antennas should not be confused with the circuit power consumption during reception and transmission drawn from the MT's battery or the BS's mains supply.

2.3 Circuit Energy Models

Power consumed at the BS and MT during transmission constitutes not only the transmission power but also the circuit power. Let us consider the case for N_T transmit and N_R receive antennas. In this paper it is assumed 4 transmit antennas at the BS, 2 receive antennas at the MT and 4 transmit antennas at the MT unless otherwise stated. Also, in addition to the parameters defined in section 2.2 above, let us define some additional parameters that will be used in the power consumption analysis: $P_{L,Rx}$ the power consumed by the MT during reception on the LR link, $P_{S,Rx}$ the power consumed by the MT during reception on the SR link, $P_{S,Tx,kj}$ the power consumed by the MTk while transmitting to MTj on the SR links, $P_{S,Tx,0}$ the power consumed by the circuitry of the MTs during transmission on the SR links, $P_{L,Tx,0}$ the power consumed by the circuitry of the MTs during transmission on the LR links, $P_{L,Tx,BS,0}$ the power consumed by the circuitry of the BS during transmission on the LR links and $P_{t,kj}$ the power transmitted over the air interface on the SR links from MTk to MTj.

For the purpose of this thesis, a $M - QAM$ system is assumed such that the Peak to Average ratio (PAR) will be given by $\xi = 3\frac{M-2\sqrt{M}+1}{(M-1)}$ [16]. The total power consumption along the signal path is given by two main components: the power consumption of the power amplifiers P_{PA} and the power consumption of all other circuit blocks P_{cir}. The power consumed by the power amplifiers is related to the transmit power P_{out} by the following equation [16]:

$$P_{PA} = (1 + \alpha)P_{out}. \tag{2.1}$$

Where $\alpha = \frac{\xi}{\eta} - 1$ with η being the amplifier drain efficiency $\eta = P_{out}/P_{in}$ and ξ the PAR which is dependent on the modulation scheme and constellation size. P_{in} is the supply power. Equation 2.1 can then be expressed as:

$$P_{PA} = \frac{\xi}{\eta}P_{out}. \tag{2.2}$$

For the PA, the most efficient operating point is close to the maximum power or near satu-
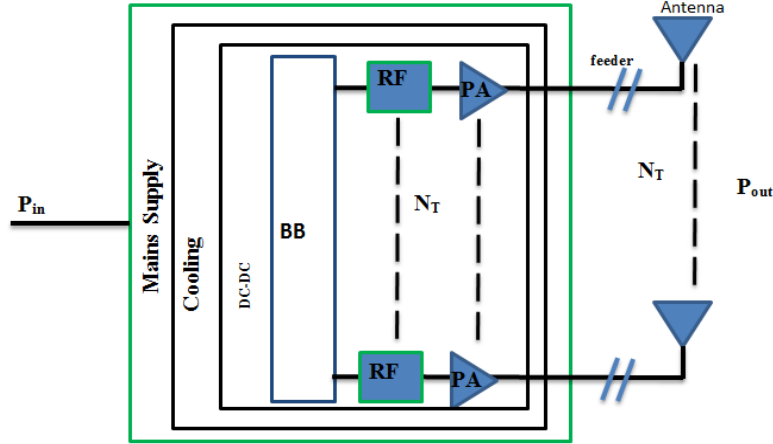
Figure 2.3: Block diagram of a base station transceiver

ration. However, non-linear effects and modulation with non-constant envelope signals force the PA to operate in a more linear region below saturation. Although this prevents adjacent channel interference due to non-linear distortion and avoids performance degradation at the receiver, this high operating back-off gives rise to poor power efficiency η. This in turn translates to higher PA power consumption P_{PA} [1]. For a BS where the PA power consumption accounts for over 50% of the energy consumption, employing techniques to improve on the power efficiency would be highly desirable. Such techniques include clipping and digital pre-distortion in combination with Doherty PAs. Silicon technologies such as Doherty and Gallium nitride (GaN) PAs have the potential to improve the efficiency and are especially suited for LTE with its high crest factor compared to GSM [17].

Circuit Power calculation at the base station during transmission on the LR link is given by:

$$P_{L,Tx,BS,0} = P_{cir:BS} + P_{sta:BS} \tag{2.3}$$

$$P_{cir:BS} = N_T (P_{dac:BS} + P_{mix:BS} + (2 \times P_{filt:BS})) + P_{syn:BS} \tag{2.4}$$

For the BS losses incurred by DC-DC power supply, main supply and active cooling scale linearly with the power consumption of the other components and may be approximated by the lossy factors
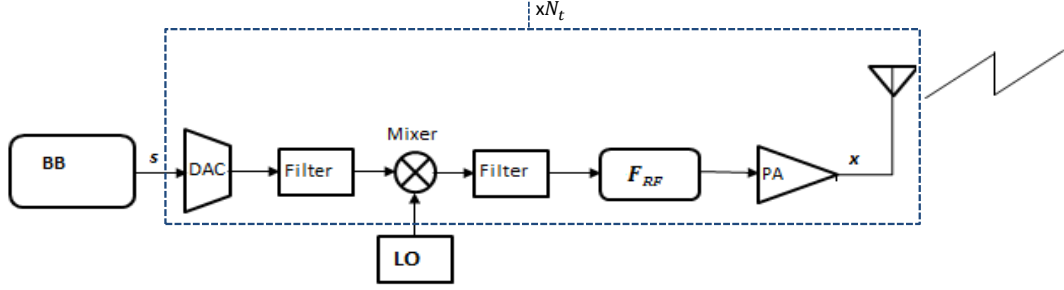
Figure 2.4: Further component break down for the Transmitter block RF chain with RF beamforming.

$\sigma_{DC:BS}$, $\sigma_{MS:BS}$, and $\sigma_{cool:BS}$, respectively [1]. The power consumption is thus modified as:

$$P_{L,Tx,BS} = \frac{\frac{\xi P_{out:BS}}{\eta(1-\sigma_{feed:BS})} + P_{L,Tx,BS,0}}{(1-\sigma_{DC:BS})(1-\sigma_{MS:BS})(1-\sigma_{cool:BS})}. \tag{2.5}$$

Note that for remote radio heads (RRH), $\sigma_{feed:BS}$ is zero due to the elimination of the feeder line.

Circuit Power calculation at the MT during transmission on the SR link is given by:

$$P_{S,Tx,0} = P_{cir:MT,Tx} + P_{sta:MT,Tx} \tag{2.6}$$

$$P_{cir:MT} = N_T(P_{dac:MT,Tx} + P_{mix:MT,Tx} + (2 \times P_{filt:MT,Tx})) + P_{syn:MT,Tx} \tag{2.7}$$

$$P_{PA:MT,Tx} = \frac{\xi P_{t,kj}}{\eta} \tag{2.8}$$

$$P_{S,Tx,kj} = P_{S,Tx,0} + P_{PA:MT,Tx} \tag{2.9}$$

Circuit Power calculation at the MT during receive on the LR link is given by:

$$P_{L,Rx} = N_R(P_{LNA,MT,Rx} + P_{mix,MT,Rx} + P_{IFA,MT,Rx} + (3 \times P_{filt,MT,Rx}) + P_{ADC,MT,Rx}) + P_{sta:MT,Rx} + P_{syn:MT,Tx}$$
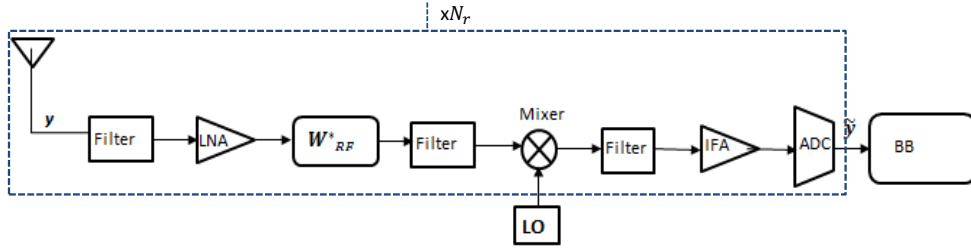
$$\tag{2.10}$$

Figure 2.5: Further component break down for the Receiver Circuit Block RF chain with RF post processing.

Circuit Power calculation at the MT during receive on the SR link is given by:

$$P_{S,Rx} = N_R(P_{LNA,MT,Rx} + P_{mix,MT,Rx} + P_{IFA,MT,Rx} + (3 \times P_{filt,MT,Rx}) + P_{ADC,MT,Rx}) + P_{sta:MT,Rx} + P_{syn:MT,Tx}$$

(2.11)

For the circuit power models used in this paper, it is assumed that the receiver gain adjustment is performed solely in the IFA. Therefore the power consumption values for the filters, LNA, frequency synthesizers and mixers can be approximated as constants and are quoted from several publications as given in chapter 4. Although the power consumption for the IFA is dependent on the receiver gain, which varies along the channel conditions, it is approximated as a constant since it is much smaller than P_{syn} or P_{LNA} in the model used [13]. Power consumption for the DACs and ADCs are obtained from the models used in [13], where it is assumed that a binary-weighted current-steering DAC is used and an estimation model for evaluating the power consumption of Nyquist-rate ADCs is used.

2.4   Beamforming and Data Rates

In wireless communication systems beamforming can be performed at the RF path, LO path, Baseband path or the digital path. In this paper we will look at beamforming performed at the RF path which offers some advantages when compared with beamforming at the baseband path. Unlike
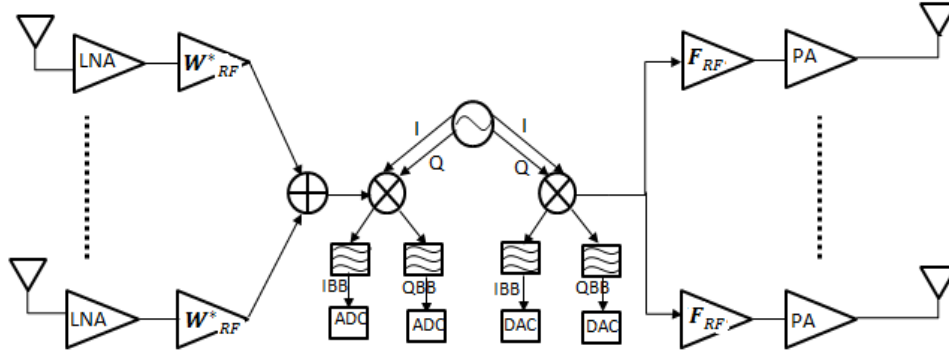
14

Figure 2.6: RF-Path beamforming

baseband beamforming where the phase shift can be achieved by four variable gain amplifiers in the transmit/receive chain, RF beamforming requires two VGAs which will translate in power savings for the system [18]. Therefore RF beamforming offers lower component count and less circuit complexity. Additionally, it is highly suitable for use in millimeter and sub millimeter wave systems which are used in current and proposed future MIMO systems. In figure 2.7 we see a typical MIMO beamforming architecture where the beam forming is performed in the digital domain. This has several draw backs as mentioned in [19] and [18] due to multiple ADC and DAC for each array element leading to increased power consumption as a direct result of the additional number of high speed ADCs and DACs.

In this paper, to isolate the problem of system performance from that of channel estimation we will assume that the channel state information (CSI) is perfectly know at both the receiver and transmitter. At any time instant t, the discrete-time transmitted signal is given by $\mathbf{x} = \mathbf{F_{RF}s}$ where $\mathbf{s}$ is the $N_s X 1$ symbol vector and $\mathbf{F_{RF}}$ the RF precoder. The received signal is thus given by:

$$\mathbf{y} = \mathbf{Hx} + \mathbf{n} \tag{2.12}$$

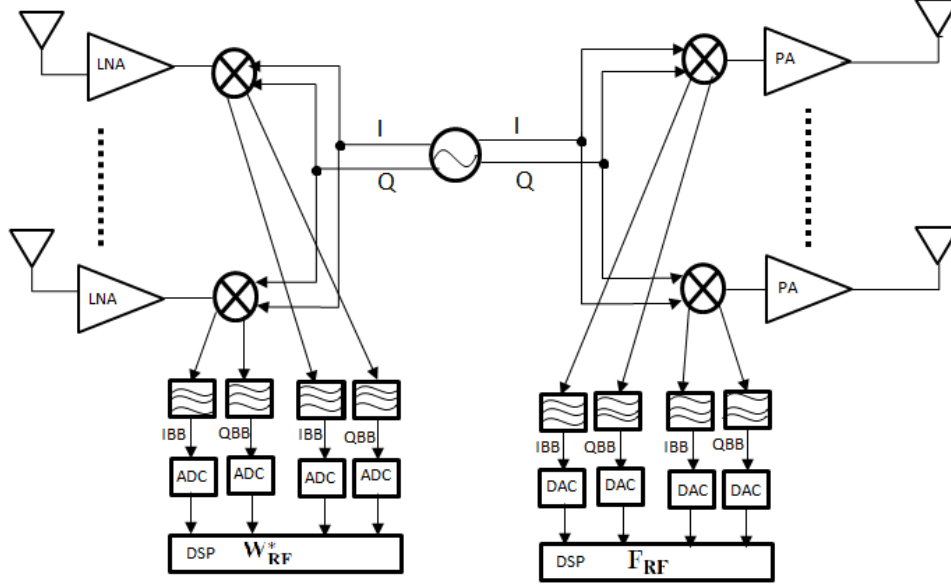or

$$\mathbf{y} = \mathbf{HF_{RF}s} + \mathbf{n}. \tag{2.13}$$

Figure 2.7: Digital beamforming in the DSP unit

Where $\mathbf{y}$ is the $N_R X 1$ received vector, $\mathbf{H}$ is the $N_R X N_T$ channel matrix, and $\mathbf{n}$ is the noise vector which is i.i.d and $CN(\mathbf{0}, \sigma_\mathbf{n}^2)$. The RF precoder $\mathbf{F_{RF}}$ and post processing $\mathbf{W_{RF}^*}$ matrices are obtained from the singular value decomposition (SVD) of the channel matrix $\mathbf{H}$ and is illustrated in figure 2.8. This is possible due to the assumption made that CSI is known at both the transmitter and the receiver. The SVD of $\mathbf{H}$ is given by:

$$\mathbf{H} = \mathbf{U} \wedge \mathbf{V}^*. \tag{2.14}$$

Where $\mathbf{U} \in \mathscr{C}^{(N_R X N_R)}$ and $\mathbf{V} \in \mathscr{C}^{(N_T X N_T)}$ are (rotation) unitary matrices and $\wedge \in \mathscr{C}^{(N_R X N_T)}$ is a diagonal matrix whose elements are nonnegative real numbers and off-diagonal elements are zero [20]. The post processing received signal is thus given by:

$$\tilde{\mathbf{y}} = \mathbf{W_{RF}^* H F_{RF} s} + \mathbf{W_{RF}^* n}. \tag{2.15}$$

Where $\tilde{\mathbf{y}}$ is the post processing received signal given by $\tilde{\mathbf{y}} = \mathbf{U}^* \mathbf{y}$, $\tilde{\mathbf{x}} = \mathbf{s} = \mathbf{V}^* \mathbf{x}$, $\mathbf{V}^* = \mathbf{F_{RF}^*}$, $\tilde{\mathbf{n}} = \mathbf{U}^* \mathbf{n}$ and $\mathbf{U}^* = \mathbf{W_{RF}^*}$. When Gaussian symbols are transmitted over the channel, the achievable rate or
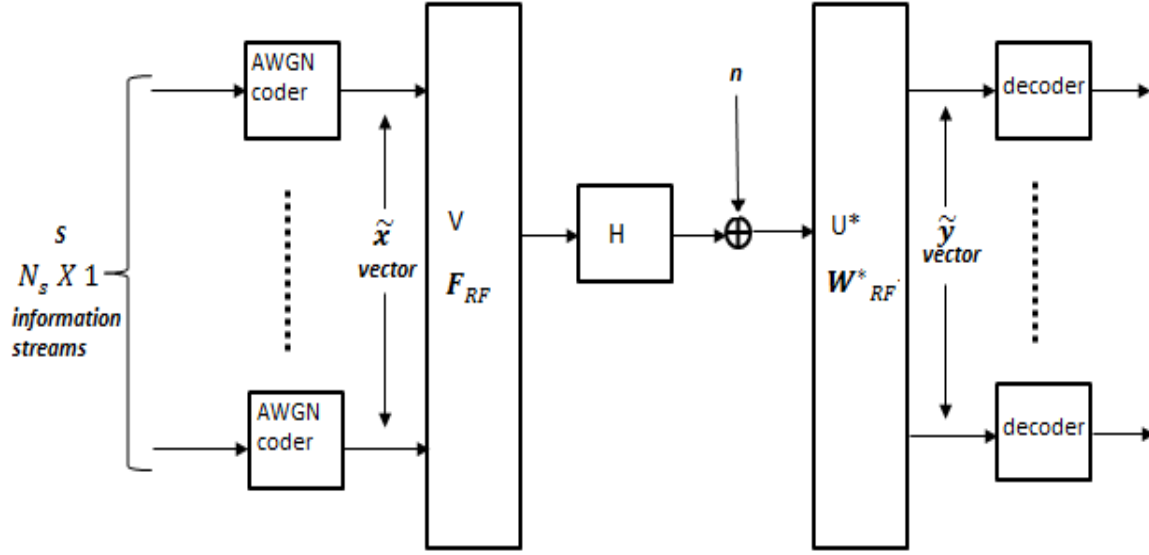
Figure 2.8: The SVD architecture for MIMO communication

spectral efficiency will be given by:

$$R = \sum_{i=1}^{i=n_{min}} B \cdot \log_2 \left(1 + \psi \frac{\rho \lambda_i^2}{N_s N_o B} \right). \qquad (2.16)$$

Where $n_{min} = min(N_R, N_T)$, λ_i^2 are the eigenvalues of the matrix $\mathbf{HH^*}$, ρ represents the average received power (we divide by N_s since we assume equal power allocation at the transmit antennas), B is the passband bandwidth of the channel and ψ is the power penalty factor associated with the M-QAM system used. It is the gap between the theoretical Shannon capacity and the spectral efficiency of a M-QAM system and is given by [21], [22]:

$$\psi = \frac{1.5}{ln(0.2/Pe)} < 1. \qquad (2.17)$$

Fading of the channel is modeled as Rayleigh fading and considered to be block fading such that Rayleigh fading remains constant for a fixed time T_{dec}, which is the channel de-correlation time. The LR and SR links are assumed to be orthogonal and are modeled by path-loss, shadowing and fading. For received power P_r it can be linked to the transmitted power P_t by the path-loss

model as in [15]:

$$\frac{P_r}{P_t}(dB) = 10\log_{10}k - 10v.\log_{10}d + h_{dB} + f_{dB}(a).$$ (2.18)

Where k is a unit less constant that depends on the antenna characteristics and the average channel attenuation, v is the path loss exponent, d is the distance where the received power is calculated, h is a Gaussian random variable representing shadowing or slow fading having a zero mean and a variance $\sigma^2_{h_{dB}}$ and f is a random variable representing Rayleigh fading with a Rayleigh parameter a.

Chapter 3

Cooperation and Energy Efficiency

3.1 AD HOC Cooperation

Having modeled the circuit powers and rate the next step is to model the proposed cooperative network. Clustering is defined as the process that divides the network into interconnected substructures called clusters. Within each cluster, a particular node is then selected as cluster head (CH) based on a specific metric or combination of metrics [23]. Clustering schemes can be classified based on their objectives and/or the cluster heads selection criteria and in [23] five classifications are proposed which are: Identifier neighbor based clustering, topology based clustering, mobility based clustering, energy based clustering and weight based clustering.

In identifier neighbor based clustering, a unique ID is assigned to each node. Each node in the network knows the ID of its neighbors. The cluster head is selected based on criteria involving these IDs such as the lowest ID, highest ID etc. In the topology based clustering, the cluster head is chosen based on a metric computed from the network topology like node connectivity. In Mobility Based Clustering, relative mobility of nodes is used as a criterion in the cluster head selection. The idea is to choose nodes with low mobility as cluster heads because they provide more stability [23]. In Energy based Clustering, the residual battery power of nodes is considered since the battery power of a node is a constraint that affects directly the lifetime of the network, hence the

energy limitation poses a severe challenge for network performance. In Weight based clustering techniques, a combination of weighted metrics such as: transmission power, circuit power, node degree, distance difference, mobility and battery power of mobile nodes etc, are considered in CH selection such that the weighting factors can be adjusted for different scenarios [23]. From the analysis in [23] it is observed that the total overhead increases when the number of nodes in a cluster is high and CHs change frequently. The weight based clustering scheme performs better than ID-Neighbor based, topology based, mobility based and energy based clustering. It is no surprise then that the weight based clustering scheme is the most used technique for CH selection where, combined weight metrics such the node degree, remaining battery power, transmission power, circuit power, and node mobility etc can be considered [23]. This scheme is thus able to achieves several goals of clustering such as: minimizing the number of clusters, maximizing lifespan of mobile nodes in the network, decreasing the total overhead, minimizing the CHs change frequency, decreasing the number of re-affiliation, improving the stability of the cluster structure and ensuring good resource management [23].

In this paper we use a form of weight based clustering scheme where nodes (referred to as MTs) in the cluster are determined by MTs interested in the same content and proximity to one another. CH selection is based on minimizing the total power consumption for the cluster. To ensure fairness in CH selection so that no one MT/node has its battery excessively drained, CH selection is done on every channel realization as channel conditions between MTs in the cluster change. Cluster formation is illustrated in figure 3.1. In this, the MTs perform cooperative Point to Point (P2P) collaboration in a distributed way with a partial control from the BS in the final step to avoid any inconsistencies in cluster formation. For the purpose of this paper, cluster formation is as follows:

An MT starts by discovering its neighbors on the SR wireless technologies supported by its SR wireless interfaces. If a neighbor is detected, the MT checks if it is allowed by the network to perform cooperative content distribution with it. This constitutes a subscription for such a service with the mobile operator to allow the BS track the content distribution to the MTs since not all
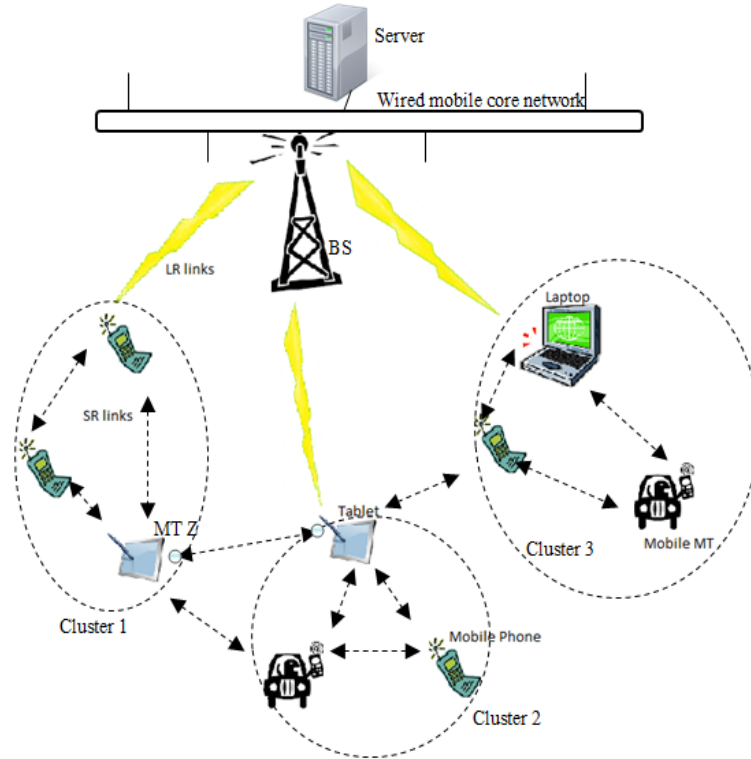
Figure 3.1: Cluster formation

the MTs will be receiving the content on the LR cellular links [15]. Also users having different interest can subscribe to different services. After making sure the neighbor MT is allowed to perform P2P collaboration and is interested in the same content, the MT initiating the neighbor discovery process should make sure that the neighbor is willing to cooperate. Privacy concerns also necessitate the need for users to be able to activate or deactivate the cooperation functionality of the MTs. After an MT has discovered a neighbor subscribed to the same service and willing to cooperate, achievable data rates via SR communication are estimated, for example, by exchanging pilot signals to estimate the CSI on their common communication link [15], [10]. After all possible neighbors are discovered, each MT sends to the BS a list of the discovered neighbors, if any, along with the achievable data rates on the communication links with each neighbor. The CSI on the LR links can be estimated via CSI feedback. With this information, the BS can group neighboring MTs into collaborative clusters and the intervention of the BS helps to avoid having a MT as a member in more than one cluster. In fact, considering the example of figure 3.1, MTZ can be part

21

of Cluster 1 or 2. However, the BS intervention breaks the confusion and specifies the members of each cluster [15].

To overcome the problem of high overhead due to the need to establish CSI in the SR links, a cluster head scenario is employed where the BS needs only CSI on the LR link with the cluster head (CH). The CH then broadcasts pilot signals to the MTs. These pilot signals are then used by the MTs to determine the CSI on the SR link with the CH. It is this CSI that is then used by the CH to determine the achievable rates of the MTs on the SR links. Thus instead of having each MT exchange CSI on the SR with (K-1) other MTs, it only exchanges information with one MT, the CH [15]. For the purpose of this paper, I will focus on one cluster to investigate the cooperative strategy that achieves minimal energy consumption and high energy efficiency within the cluster.

3.2   Energy Minimization

In this section I will consider the energy minimization problem with unicasting on the LR and multicasting in the SR using the circuit power models and rate equations already derived in the previous sections. For K requesting MTs that are intending to download common content from a centralized location (such as a server on the internet) in a cooperative manner , the time t_k taken to send d_k bits over a link with rate R_k is $t_k = d_k/R_k$. Using the general energy formula $E = P.t$ where P is the power consumption and t time spent in transmission or reception, the energy $E_{coop,k}$ consumed when MTk is selected as the CH is given by:

$$E_{coop,k} = \frac{S_T}{R_{L,k}}P_{L,Tx} + \frac{S_T}{R_{L,k}}P_{L,Rx} + S_T.\frac{P_{S,Tx,k}}{\min_{i\neq k}R_{S,ki}} + S_T.\frac{\sum\limits_{j=1,j\neq k}^{K}P_{S,Rx,j}}{\min_{i\neq k}R_{S,ki}}. \qquad (3.1)$$

Where the first term represents the energy consumed by the base station during transmission to MTk the second term represents the energy consumed by MTk during reception on the LR link, the third term corresponds to the energy consumed by MTk to transmit the data on the SR link, and the last term represents the energy consumed by the other MTs during reception of the data

from MTk on the SR link. For the case of SR multicasting by the CH, MTk will transmit using the minimum achievable rate with the MTs in the same cooperative cluster. Rate adaptive transmission is assumed where the MT total transmit power is constant meaning $P_{t,k,j} = P_t$ and $P_{S,Tx,kj} = P_{S,Tx}$. Thus the rate $R_{S,kj}$ on the link between MTk and j is the rate achievable with the transmit power P_t and is varied adaptively depending on the channel condition between the MTk and j [15].

Assuming MTs have the same SR wireless interfaces, the SR power consumption during reception of data will be the same for all MTs therefore $P_{S,Rx,j} = P_{S,Rx} \forall j$. Therefore 3.1 can be simplified as:

$$E_{coop,k} = \frac{S_T}{R_{L,k}} P_{L,Tx,BS} + \frac{S_T}{R_{L,k}} P_{L,Rx} + S_T . \frac{P_{S,Tx,k}}{\min_{i \neq k} R_{S,ki}} + S_T . (K-1) \frac{P_{S,Rx}}{\min_{i \neq k} R_{S,ki}}. \tag{3.2}$$

For the case of no cooperation between the MTs, and the BS unicasts the content on the LR links to each MT, the total energy consumption for this case would be given by:

$$E_{No-coop-U} = \sum_{k=1}^{K} \left(\frac{S_T}{R_{L,k}} P_{L,Tx,BS} + S_T \frac{P_{L,Rx,k}}{R_{L,k}} \right) \tag{3.3}$$

For the case of no cooperation between the MTs, and the BS multicasts the content on the LR links using the rate achievable by the MT having the worst channel conditions to each MT, the total energy consumption for this case would be given by:

$$E_{No-coop-M} = \frac{S_T}{\min_j R_{L,j}} P_{L,Tx,BS} + S_T \frac{\sum_{j=1}^{K} P_{L,Rx,j}}{\min_j R_{L,j}}. \tag{3.4}$$

To indicate whether the cooperation is beneficial or not with regards to energy consumption, the normalized energy consumption θ is defined as:

$$\theta = \frac{E_{coop,k}}{E_{No-coop-U}}. \tag{3.5}$$

If $\theta < 1$, the cooperation offers improved energy consumption else if $\theta > 1$ indicates a non-

beneficial cooperation in terms of energy consumption savings. To minimize the total energy consumption of the MTs forming a single cooperating cluster, the optimal solution with LR unicasting consists of a CH set up. Here all the data is sent to the CH on the LR link and the CH distributes the content to the other MTs in the cluster on the SR links. The BS selects the CH k^* as relay that minimizes the energy consumption where k^* is given by equation 3.6 given that equation 3.2 is satisfied [15]:

$$k^* = \arg\min_k \left(\frac{P_{L,Tx,BS}}{R_{L,k}} + \frac{P_{L,Rx}}{R_{L,k}} + \frac{P_{S,Tx,k} + (K-1)P_{S,Rx}}{\min_{i \neq k} R_{S,ki}} \right). \tag{3.6}$$

So far equations 3.1 to 3.6 have assumed that the LR and SR rates were fixed during the entire data distribution process. Such a scenario would occur for the case of low to moderate mobility of the MTs. For fast fading scenarios, the channel might change before the entire content is distributed. In such a situation, for each T_{dec}, the BS should select the CH k^* that would minimize the energy consumption. The CH selected at each iteration for transmission on the SR varies due to the fading fluctuations and hence leads to fairness in energy consumption among the different MTs. The number of bits available at each channel realization m is now given by [15]:

$$S_R(m) = S_T - \sum_{y=1}^{m-1} R_{L,k^*(y)}(y).T_{dec}. \tag{3.7}$$

During T_{dec}, the amount of bits sent to k^* will either be $R_{L,k^*(m)}(m).T_{dec}$ or $S_R(m)$ if the remaining data bits are less than the amount that can be transmitted during the mth channel realization [15].

Equations 3.2 and 3.6 are therefore modified to give the total energy and the MT selected to minimize the energy consumption during each fading realization in the cooperative cluster as shown below:

$$E_{coop,k}(m) = \left(R_{L,k^*(m)}(m).T_{dec}, S_R(m) \right).\left(\frac{P_{L,Tx,BS}}{R_{L,k}(m)} + \frac{P_{L,Rx}}{R_{L,k}(m)} + \frac{P_{S,Tx,k}}{\min_{i \neq k} R_{S,ki}(m)} + (K-1)\frac{P_{S,Rx}}{\min_{i \neq k} R_{S,ki}(m)} \right) \tag{3.8}$$

and

$$k^*(m) = \arg\min_k \left(\frac{P_{L,Tx,BS}}{R_{L,k}(m)} + \frac{P_{L,Rx}}{R_{L,k}(m)} + \frac{P_{S,Tx,k} + (K-1)P_{S,Rx}}{\min_{i \neq k} R_{S,ki}(m)} \right). \tag{3.9}$$

The overall energy efficiency is then defined as $EE_{coop} = \frac{E_{coop}}{R}$ in joules per bit for the cooperative case and $EE_{No-coop} = \frac{E_{No-coop}}{R}$ for the non-cooperative case. In this case R is taken to be the average rate for the given scenario.

Chapter 4

Simulation and Analysis

Simulation is done to obtain the total energy consumption and the normalized energy consumption for the proposed system model. Also the energy efficiency (EE) and the energy efficiency gain are analyzed. Matlab is used as the simulation platform as it is one of the most widely used tools for physical layer modeling of wireless systems. It also has a variety of digital communication blocks and analyzing tools available for evaluating system performance [24]. The MTs in a cluster are assumed to be randomly distributed in a 20m X 20m area with the LR BS link originating at a distance of 400 m from the center of the cluster. Simulation parameters used are shown in table 4.1 where the energy consumption parameters are taken from [24], [5], [8] for the MT and those for the BS are taken from [1]. The channel parameters used are for 4G LTE systems and are obtained from [25], [10], [15].

4.1 Results Evaluations

Performance is compared in terms of energy reduction for cooperative SR multicast, cooperative SR Unicast, non-cooperative unicast and non-cooperative multicast scenarios. Figure 4.1 shows the normalized energy results for SR unicasting, SR multicasting and non-cooperative multicasting. Normalization is done with respect to energy consumption for non-cooperative unicasting. It is observed from figure 4.1 that cooperation out performs non-cooperative unicasting since the value

Table 4.1: Simulation Parameters

| Parameter	Value
SR bandwidth	1MHz
LR bandwidth	10MHz
Long range distance (D_{LR})	400m
Pathloss constant (k)	-128.1dB
Channel decorrelation time (T_{dec})	10ms
Pathloss exponent (Shadowed urban) (v)	3.76
Shadowing standard deviation (σ_{h_dB})	8dB
Bit error rate (P_e)	10^{-6}
Content size (S_T)	1Mbits
Receiver noise figure	7dB
Main power supply lossy factor BS ($\sigma_{MS:BS}$)	9%
Active cooling system lossy factor BS ($\sigma_{cool:BS}$)	10%
$DC - DC$ power supply lossy factor BS ($\sigma_{DC:BS}$)	7.5%
Lossy factor of antenna feeder BS ($\sigma_{feed:BS}$)	3dB, 0 for RRH
Baseband interface power consumption BS ($P_{sta:BS}$)	14.6W
RF chain power consumption BS ($P_{cir:BS}$)	10.9W
PA power consumption BS ($P_{PA:BS}$)	51.5
BS transmit power on LR ($P_{out:BS}$)	20W
MT transmit power on SR ($P_{out:MT,Tx}$)	0.13W
MT PA efficiency	35%
MT DAC power consumption ($P_{dac:MT,Tx}$)	15.5mW
MT ADC power consumption ($P_{adc:MT,Tx}$)	9.8mW
MT filter power consumption ($P_{filt:MT}$)	2.5mW
MT frequency synthesizer power consumption ($P_{syn:MT}$)	50mW
MT idle/static power consumption (BB interface) ($P_{sta:MT}$)	15mW
MT mixer power consumption ($P_{mix:MT}$)	30.3mW
MT LNA power consumption ($P_{LNA:MT}$)	20mW
MT IFA power consumption ($P_{IFA:MT}$)	3mW
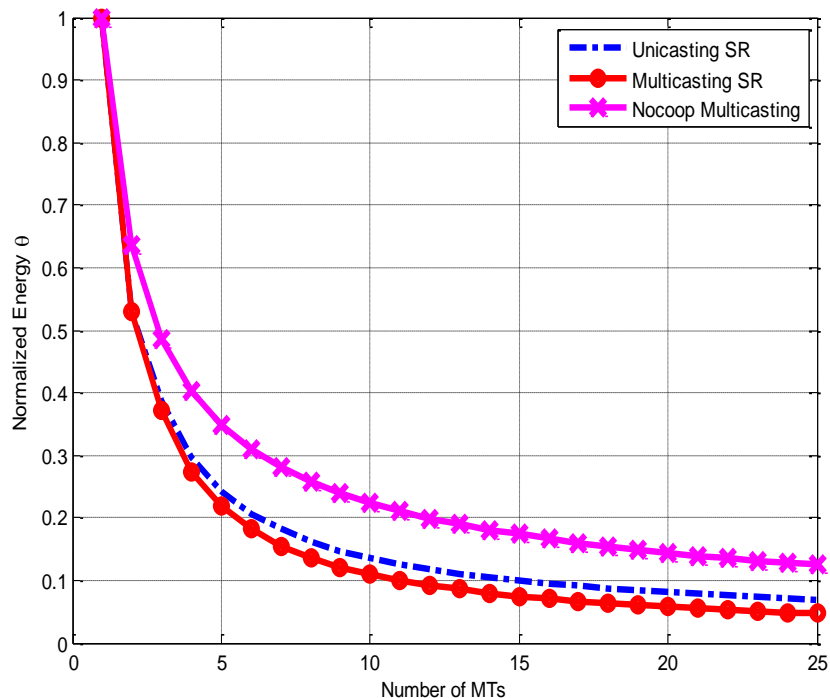
Figure 4.1: Normalized energy consumption vs number of MTs (4X2 MIMO)

of θ where $\theta = E_{coop,k}/E_{No-coop-U}$ is less than one and SR cooperative multicasting outperforms both non-cooperative multicasting and SR cooperative unicasting.

Comparing the un-normalized energy consumption for all scenarios in figure 4.2 we can see more clearly the energy saving advantages for cooperation. It is observed that both cooperative SR multicasting and cooperative SR unicasting outperform the non-cooperative scenarios. This result is expected since in the non-cooperative unicasting case the BS transmits to each MT individually and MTs receive data on their LR links only. For the case of non-cooperative multicasting the MTs will also keep their LR interfaces active to receive the data from the BS. For the cooperative case, the BS transmits on the LR link to the CH only. If retransmission is done via SR unicasting then the CH will retransmit to each MT interested in the same data individually. However, if SR multicasting is used during retransmission then the CH transmits all at once to all MTs interested in the same content, hence lower energy consumption is observed for the cooperative SR multicasting scenario. While figure 4.2 analyses the unnormalized energy consumption for the different
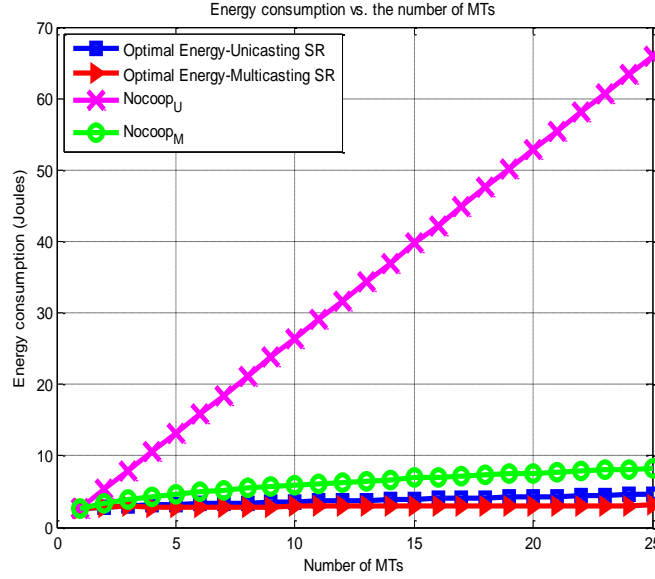
Figure 4.2: Energy consumption vs number of MTs (4X2 MIMO)

scenarios figure 4.3 shows the analysis of the EE metric defined in chapter 3. Figure 4.3 shows that cooperative SR multicasting is the most efficient of the four scenarios evaluated with a lower energy consumption per bit as the cluster size increases when compared to the other scenarios.

Defining energy efficiency gain as:

$$EE_{gain} = \frac{EE_{Scheme1} - EE_{Scheme2}}{EE_{Scheme1}}. \qquad (4.1)$$

Figure 4.4 illustartes the efficiency gain of the three scenarios; cooperative SR multicasting, cooperative SR unicasting and non-cooperative LR multicasting when compared to non-cooperative LR unicasting. From this it is observed that the gain converges to about 85% for the most energy efficient scenario of SR multicasting as the number of cooperating MTs increases. Also it is observed that having more nodes cooperating offers increased gains in energy efficiency. For example in a cluster of 5 cooperating MTs, SR multicasting has a 60% gain in efficiency when compared to a non-cooperative unicasting scenario while at 25 MTs the gain is about 85%. When the two cooperating scenarios are compared to the case of non-cooperative multicasting it is observed that the efficiency gain for the cooperative SR multicasting scenario converges at about 70% as illustrated
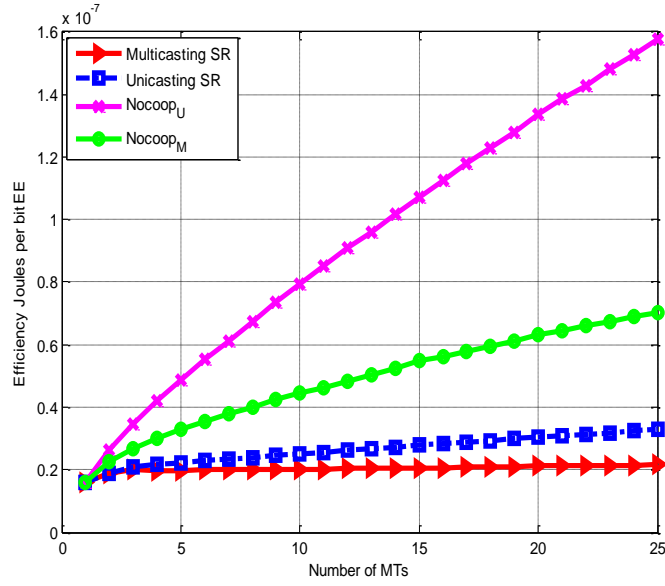
29

Figure 4.3: Energy efficiency vs number of MTs (4X2 MIMO)

in figure 4.5.

From these results we see that cooperative SR multicasting outperforms the other three scenarios in terms of energy consumption and efficiency as the number of cooperating MTs in a cluster increases from 1 MT to 25 MTs. Next in figure 4.6 the effect of MIMO on energy efficiency as the number of cooperating MTs in a single cluster increases and the number of Tx and Rx antennas increase is evaluated. From figure 4.6 it is observed that as the number of antennas increase, the energy efficiency improves. The joules per bit value decreases as the number of antennas increases and it will converges to a value since it can never get to zero. This is expected since the total circuit energy consumption will increase linearly as the number of antennas increases. This is due to the increasing number of circuit components needed to drive the additional antennas. The rate however, is a logarithmic function that increases monotonically as the number of antennas increases and can never go to infinity no-matter how large the MIMO system gets. Figure 4.6 illustrates this by the gap between the energy efficiency curves getting smaller and smaller until the curves tend to overlap as the number of antennas increase. In figure 4.7 we observe that the curves tend to converge as the number of antennas increases and the energy per bit never gets to zero. Each curve in figure 4.7 represents the energy efficiency in joules per bit as the number of transmit antennas
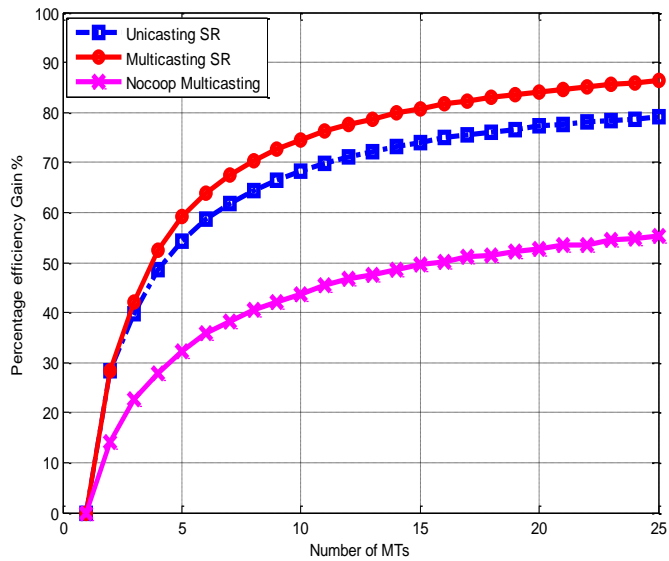
Figure 4.4: Percentage efficiency gain over Non-cooperative unicasting vs number of MTs (4X2 MIMO)
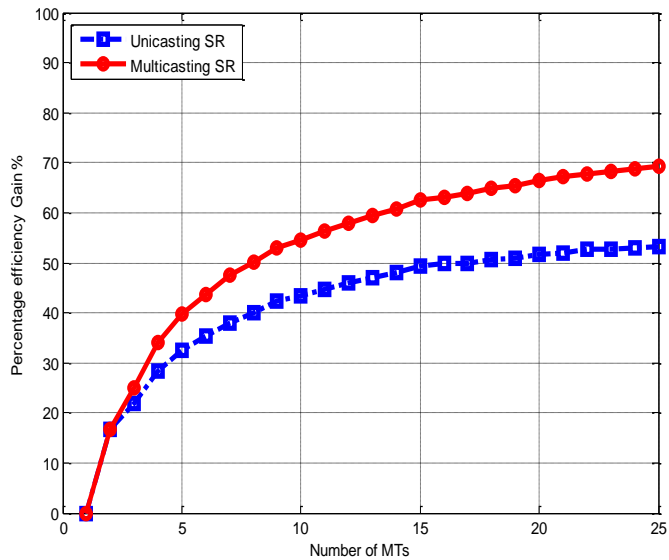

Figure 4.5: Percentage efficiency gain over Non-cooperative multicasting vs number of MTs (4X2 MIMO)
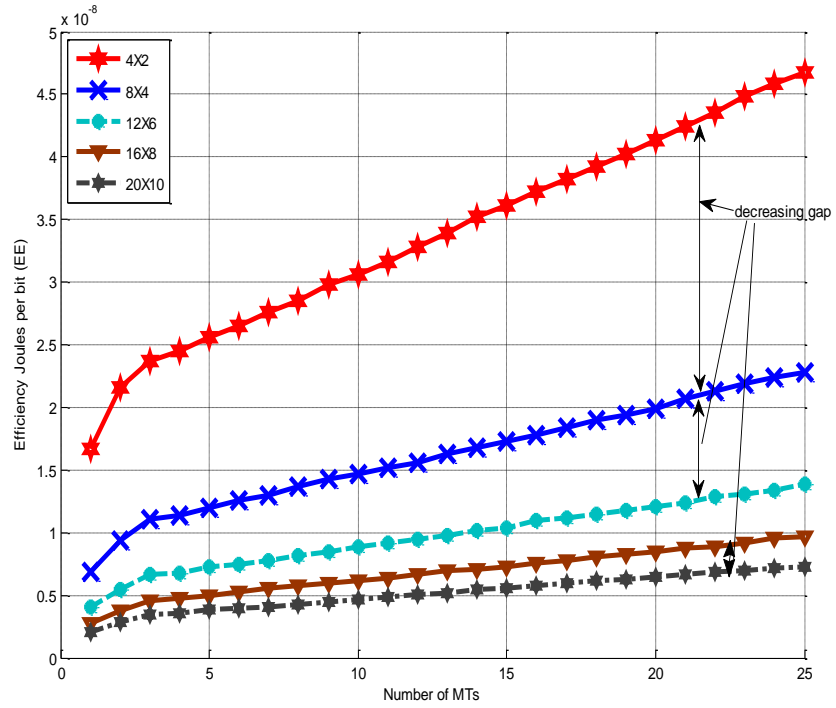
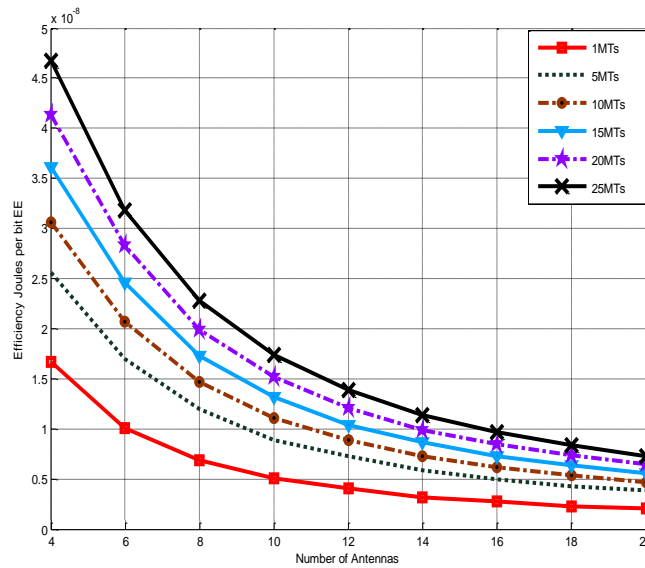Figure 4.6: Energy efficiency vs number of MTs as number of Tx and Rx antennas increases

Figure 4.7: Energy efficiency vs number of transmit antennas (N_t) for K= 2,5,10,15,20,25 cooperating MTs

increase from 2 to 20 for a fixed number of cooperating MTs in the cluster.

From these two graphs in figures 4.6 and 4.7 we can conclude that increasing the number of Tx and Rx antennas significantly improves the energy efficiency of the system.

Chapter 5

Conclusion and Future Work

In this paper I have looked at a practical power consumption model which includes circuit power from the different components in a transceiver chain. This is of great significance to practical system design when doing energy consumption and energy efficiency analysis. Based on the this power consumption model, the energy efficiency for cooperative MIMO systems was analyzed in the context of optimized energy consumption for different scenarios within a single cooperative cluster. SR multicast cooperation was found to have significant energy savings and improved energy efficiency as compared to the other scenarios. Also It was observed that increasing the number of Tx and Rx antennas for MTs within a single cooperating cluster achieved significant energy savings as illustrated in figures 4.6 and 4.7.

In this paper it was assumed that the CSI is know by the transmitter but we know that for this information to be available there needs to be additional feedback between the MTs. Accounting for this overhead and the additional overhead during cluster formation and cluster maintenance can form a basis for future works.

Cluster size management in extension to the work done in this paper is also a good area of research. With the objective of clustering algorithms being to partition the network into several clusters, optimal cluster size will be dictated by trade-offs between energy minimization, delay minimization, spatial reuse etc. Depending on which of these metrics is used, the optimal number

of cooperating MTs in a cluster can then be determined.

In this paper to avoid one MT being the CH during the entire transmission process, CH selection was done during each fading iteration. However, this setup is based solely on minimizing the total power consumption of the cluster and no consideration is given as to how much battery power is remaining for the MT selected as CH. Incorporating remaining battery power at the MT as one of the metrics in a weight based clustering scheme during CH selection can be done in conjunction with metrics used in this paper. Such a setup will not only take advantage of the energy efficiency gains of a cooperative MIMO system but will also extend the lifetime of the cooperative network.

References

[1] Energy Efficiency Analysis of the Reference Systems, Areas of Improvements and Target Breakdown. *project deliverable, D2.3*.

[2] B. Sanou. Measuring the Information Society. *International Telecommunication Union (ITU)*, February 2013.

[3] A. Fehske, G. Fettweis, J. Malmodin, and G. Biczok. The Global Footprint of Mobile Communications: The Ecological and Economic Perspective. *Communications Magazine, IEEE*, 49(8):55–62, August 2011.

[4] D. S. Hopeton. The Carbon Footprint of ICTs. *Global Information Society Watch*, 2010.

[5] D. Feng, C. Jiang, G. Lim, J. L. Cimini Jr, G. Feng, and G.Y. Li. A Survey of Energy-Efficient Wireless Communications. *Communications Surveys Tutorials, IEEE*, 15(1):167–178, First Quarter 2013.

[6] S.P. Karmore, A.R. Mahajan, and S. Kitey. Battery Monitoring and Analysis for Android Based System. In *Advanced Computing Technologies (ICACT), 2013 15th International Conference on*, pages 1–6, September 2013.

[7] G.Y. Li, Z. Xu, C. Xiong, C. Yang, S. Zhang, Y. Chen, and S. Xu. Energy-Efficient Wireless Communications: Tutorial, Survey, and Open Issues. *Wireless Communications, IEEE*, 18(6):28–35, December 2011.

[8] C. Shuguang, A. J. Goldsmith, and A. Bahai. Energy-Efficiency of MIMO and Cooperative MIMO Techniques in Sensor Networks. *Selected Areas in Communications, IEEE Journal on*, 22(6):1089–1098, August 2004.

[9] H. Kim, C. Chan-Byoung, G. de Veciana, and R.W. Heath. A Cross-Layer Approach to Energy Efficiency for Adaptive MIMO Systems Exploiting Spare Capacity. *Wireless Communications, IEEE Transactions on*, 8(8):4264–4275, August 2009.

[10] L. Liu, R. Chen, S. Geirhofer, K. Sayana, Z. Shi, and Y. Zhou. Downlink MIMO in LTE-Advanced: SU-MIMO vs. MU-MIMO. *Communications Magazine, IEEE*, 50(2):140–147, February 2012.

[11] B. Clerckx, H. Lee, Y. Hong, and G. Kim. A Practical Cooperative Multicell MIMO-OFDMA Network Based on Rank Coordination. *Wireless Communications, IEEE Transactions on*, 12(4):1481–1491, April 2013.

[12] Z. Xu, G.Y. Li, C. Yang, S. Zhang, Y. Chen, and S. Xu. Energy-Efficient Power Allocation for Pilots in Training-Based Downlink OFDMA Systems. *Communications, IEEE Transactions on*, 60(10):3047–3058, October 2012.

[13] C. Shuguang, A.J. Goldsmith, and A. Bahai. Energy-Constrained Modulation Optimization. *Wireless Communications, IEEE Transactions on*, 4(5):2349–2360, September 2005.

[14] G. Miao, N. Himayat, and G.Y. Li. Energy-Efficient Link Adaptation in Frequency-Selective Channels. *Communications, IEEE Transactions on*, 58(2):545–554, February 2010.

[15] R. Atat, E. Yaacoub, M. Alouini, and A. Abu-Dayya. Cooperative Relay-Based Multicasting for Energy and Delay Minimization. In *Wireless Communications and Mobile Computing Conference (IWCMC), 2012 8th International*, pages 808–813, August 2012.

[16] K. J. Sudharman. Energy Analysis of MIMO Techniques in Wireless Sensor Networks. *38th conference on information sciences and systems*, 2004.

[17] O. Arnold, F. Richter, G. Fettweis, and O. Blume. Power Consumption Modeling of Different Base Station Types in Heterogeneous Cellular Networks. In *Future Network and Mobile Summit, 2010*, pages 1–8, June 2010.

[18] A. S. Y. Poon and M. Taghivand. Supporting and Enabling Circuits for Antenna Arrays in Wireless Communications. *Proceedings of the IEEE*, 100(7):2207–2218, July 2012.

[19] J. Kyung-Tae, K. Young-Chai, and Y. Hong-Chuan. RF Beamforming Considering RF Characteristics in MIMO System. In *Information and Communication Technology Convergence (ICTC), 2010 International Conference on*, pages 403–408, November 2010.

[20] D. Tse and P. Viswanath. *Fundamentals of Wireless Communication*. Wiley series in telecommunications. Cambridge University Press, 2005.

[21] Z. Zhou, B. Vucetic, M. Dohler, and Y. Li. MIMO Systems With Adaptive Modulation. *Vehicular Technology, IEEE Transactions on*, 54(5):1828–1842, September 2005.

[22] A. Goldsmith. *Wireless Communications*. Cambridge University Press, 2005. Cambridge Books Online.

[23] A. Bentaleb, A. Boubetra, and S. Harous. Survey of Clustering Schemes in Mobile Ad hoc Networks. *Communications and Network*, 5(2B):8–14, May 2013.

[24] Z. Rafique, B.C. Seet, and A. Al-Anbuky. Performance Analysis of Cooperative Virtual MIMO Systems for Wireless Sensor Networks. *PMC free article PubMed Sensors*, 13:7033–7052, June 2013.

[25] F. Khan. *LTE for 4G Mobile Broadband: Air Interface Technologies and Performance*. Cambridge University Press, 2009.